Conversion of a Metastable Superhydrophobic Surface to an Ultraphobic Surface

Xue-Mei Li,*[,†,‡] Tao He,[†] Mercedes Crego-Calama,[‡] and David N. Reinhoudt*[,‡]

State Key Laboratory of Materials-Oriented Chemical Engineering, College of Chemistry and Chemical Engineering, Nanjing University of Technology, 5 Xinmofan Road, China, 21009, and Laboratory of Supramolecular Chemistry and Technology Group, MESA+ Institute for Nanotechnology, University of Twente, P.O. Box 217, 7500AE Enschede, The Netherlands

Received April 3, 2008. Revised Manuscript Received May 13, 2008

Superhydrophobic surfaces in Wenzel and metastable wetting state were prepared and the conversion of such surfaces to ultraphobic surfaces was reported by the application of a fine-scale roughness. Silicon nitride substrates with hexagonally arranged pillars were prepared by micromachining. The two-scale roughness was achieved by coating these substrates with 60 nm silica nanoparticles. The surface was made hydrophobic by silanization with octadecytrichlorosilane (OTS). Wettability studies of the silicon nitride flat surface, silicon nitride pillars, and the surfaces with two-scale roughness showed that a two-scale roughness can effectively improve the hydrophobicity of surfaces with a higher apparent contact angle and reduced contact angle hysteresis when the original rough surface was in a metastable or Wenzel state. This study shows the pathway of converting a metastable hydrophobic surface to an ultraphobic surface by the introduction of a fine-scale roughness, which adds to the literature a new aspect of fine-scale roughness effect.

Introduction

Surfaces with very high water contact angle (≥150°) are considered superhydrophobic.[1] Because of the very little contact between the superhydrophonic surface and a water droplet, the superhdrophobic surfaces show little adhesion to the water droplet and self-cleaning effects are expected when the droplet rolls off the surface, meanwhile taking away dust particles. There is great interest in the preparation of superhydrophobic surfaces, and many methods have been developed and reviewed.[1–4]

Studies have shown that a rough surface is a fundamental requirement for the preparation of a suyperhydrophobic surface. A water droplet can be suspended on top of the asperities or wet the groove among the asperities on superhydrophobic surfaces. These two states of wetting are referred as composite and collapsed, respectively. Many research groups have observed the transition from the composite to a collapsed state upon external disturbance on artificial superhydrophobic surfaces.[5–10] The composite wetting is, therefore, observed as a metastable state. In most cases, a transition from the suspended drop to a collapsed drop is energetically more favorable. When this transition took place, a lower water contact angle is observed, leading to less hydrophobic surfaces. Moreover, in the collapsed drop, significant pinning of water to the groove is observed, leading to significant increase in the contact angle hysteresis, which makes the surface sticky and the rolling off of a water droplet difficult, thus affecting the overall superhydrophobicity of the substrates. Therefore, it is important to find a method to fabricate a stable superhydrophobic surface, i.e. an ultraphobic surface.[11]

Recent studies in mimicking lotus leaf structure have revealed that surfaces with hierarchical structures show unusual water repellency.[10,12–19] Hierarchical structure is also referred as two-scale roughness. It has been shown that the introduction of fine-scale roughness can reduce the contact angle hysteresis by inhibiting water pinning among the grooves of the asperities.[12,19] However, it is not known whether the fine-scale roughness can also improve the surface superhydrophobicity in improved water contact angles. This report focused on the fine-scale roughness effect for surfaces of Wenzel and metastable wetting state. Surfaces with hierarchical structure were prepared on the basis of silicon nitride pillared substrate with a coating of silica nanoparticles. Fine-scale roughness effects were evaluated both on the apparent contact angle and contact angle hysteresis for the generation of ultraphobic surfaces.

Experimental Section

Chemicals. Octadecytrichlorosilane (OTS), tetraethylorthosilicate (TEOS), dodecytriethoxysilane (DTS) from Acros Organics, and 1*H*,1*H*,2*H*,2*H*-perfluorodecyltriethoxysilane (FDTS) from Lancaster were used as received. Aqueous ammonia was obtained from Merk Co. Solvents are of reagent grade and used as received. Silica nanoparticles were prepared following published procedures.[20]

* Corresponding author. Tel: +86-25-83587775. E-mail: xuemeili@njut.edu.cn; d.n.reinhoudt@tnw.utwente.nl.

† Nanjing University of Technology.

‡ University of Twente.

(1) Li, X.-M.; Reinhoudt, D. N.; Crego-Calam, M. *Chem. Soc. Rev.* **2007**, *36*, 1350.

(2) Sun, T. L.; Feng, L.; Gao, X. F.; Jiang, L. *Acc. Chem. Res.* **2005**, *38*, 644.

(3) Zhang, X.; Shi, F.; Niu, J.; Jiang, Y.; Wang, Z. *J. Mater. Chem.* **2008**, *18*, 621.

(4) Roach, P.; Shirtcliffe, N. J.; Newton, M. I. *Soft Matter* **2008**, *4*, 224.

(5) Patankar, N. A. *Langmuir* **2004**, *20*, 7097.

(6) Bico, J.; Marzolin, C.; Quere, D. *Europhys. Lett.* **1999**, *47*, 220.

(7) Maleki, M.; Reyssat, E.; Quere, D.; Golestanian, R. *Langmuir* **2007**, *23*, 10116.

(8) Lafuma, A.; Quere, D. *Nat. Mater.* **2003**, *2*, 457.

(9) Quere, D.; Lafuma, A.; Bico, J. *Nanotechnology* **2003**, *14*, 1109.

(10) Feng, L.; Li, S. H.; Li, Y. S.; Li, H. J.; Zhang, L. J.; Zhai, J.; Song, Y. L.; Liu, B. Q.; Jiang, L.; Zhu, D. B. *Adv. Mater.* **2002**, *14*, 1857.

(11) Extrand, C. W. *Langmuir* **2002**, *18*, 7991.

(12) Gao, L.; McCarthy, T. J. *Langmuir* **2006**, *22*, 2966.

(13) Shirtcliffe, N. J.; McHale, G.; Newton, M. I.; Chabrol, G.; Perry, C. C. *Adv. Mater.* **2004**, *16*, 1929.

(14) Patankar, N. A. *Langmuir* **2004**, *20*, 8209.

(15) Li, Y.; Cai, W.; Duan, G. *Chem. Mater.* **2008**, *20*, 615.

(16) Li, Y.; Li, C.; Cho, S. O.; Duan, G.; Cai, W. *Langmuir* **2007**, *23*, 9802.

(17) Zhao, N.; Shi, F.; Wang, Z. Q.; Zhang, X. *Langmuir* **2005**, *21*, 4713.

(18) Ming, W.; Wu, D.; van Benthem, R.; de With, G. *Nano Lett.* **2005**, *5*, 2298.

(19) Zhu, L. B.; Xiu, Y. H.; Xu, J. W.; Tamirisa, P. A.; Hess, D. W.; Wong, C. P. *Langmuir* **2005**, *21*, 11208.

10.1021/la801044j CCC: $40.75
Published on Web 07/08/2008

Table 1. Wettability of Different Silane SAMs on Silicon Nitride

SAM	static θ (deg)	θ_{adv} (deg)	θ_{rec} (deg)
FDTS	110 ± 5	120 ± 5	90 ± 5
DTS	100 ± 2	113 ± 2	93 ± 2
OTS	107 ± 2	115 ± 2	100 ± 2

Silicon Nitride Substrates. Flat reference silicon nitride substrates were prepared by low-pressure chemical vapor deposition (SiH_2Cl_2/NH_3 = 70:18 at 850 °C, 250 mbar) of a thin layer of low stress silicon nitride (300 nm) on silicon ⟨110⟩ substrate. For silicon nitride with pillars, a thicker layer of silicon nitride (1.2 μm) was prepared following a similar route. Chromium contact masks with hexagonally arrayed holes with different diameter (d, μm) and pitch distance (p, μm) (pillar center to center distance) were made. Patterns in the photoresist were created by mask photolithography on the polished side of silicon nitride. After development, the patterns were obtained by reactive ion etching (CHF_3/O_2 = 75/25, power = 75 W, pressure = 10 mbar). A series of substrates with etch depth of 0.8 μm were prepared: d1.5p2.0, d1.5p2.5, d1.5p3.0, d2.0p3.5, and d2.0p4.0. The actual parameters of the substrates are shown in Table 3.

SAM. The flat silicon nitride substrates for SAM formation were immersed in freshly prepared piranha solution for 30 min (concentrated H_2SO_4 and 33% aqueous H_2O_2 in a 3:1 ratio). (**Caution**: *Piranha solution should be handled with caution: it has been reported to detonate unexpectedly.*) The substrates were then taken out, rinsed with copious amount of water (Millipore), blown dry, and then positioned in a vacuum desiccator for gas phase SAM formation. The samples were allowed to stay in the desiccator for 14 h, and then the vacuum was released. The substrates were taken out, sonicated in toluene for 5 min to remove grease and extra unreacted monomer, rinsed with ethanol and water, and blown dry under a stream of nitrogen. The substrates were then cured at 120 °C for 12 h.

Silica Nanoparticles Coating. Dry silica nanoparticles (5 mg) were dissolved in pure ethanol (10 mL) by ultrasonication. Flat silicon nitride substrates were coated by drop casting. The number of coatings can be varied in order to obtain layers of different thickness. Pillared substrates were coated by spin-coating the silica nanoparticle solution at 2000 rpm. The substrates after coating were allowed to dry in air and cured in an oven of 120 °C overnight before SAM formation.

Contact Angle Measurements. Water contact angles were measured on a Krüss goniometer (Contact Angle Measuring System G10) equipped with a CCD camera. The advancing and receding contact angles were measured during the growth and shrinkage of a droplet, respectively. Static angle was measured in a sessile drop mode.

Field Emission Scanning Electron Microscopy (FESEMS). FESEM images were taken with a LEO 1550 field emission scanning electron microscope (Carl Zeiss Inc.).

Results and Discussion

Silicon nitride substrates were prepared by low-pressure chemical vapor deposition. Silica nanoparticles were prepared following published methods.[20] Specifically, tetraethylorthosilicate (TEOS) was hydrolyzed and condensed in the presence of ammonia in ethanol. The ratio between TEOS and ammonia determines the final particle size. Particles of with diameters of 60 nm were prepared.

Self-Assembled Monolayer on Silicon Nitride. Self-assembled monolayers of the different silanization reagents OTS, DTS, and FDTS were prepared by gas-phase deposition. The wettability of a surface is characterized by the water contact angle (CA). Both static CA (θ) and dynamic CAs ($\theta_{adv}/\theta_{rec}$) were determined. A static CA shows the basic wetting property (hydrophilic or hydrophobic) of a surface, while the dynamic

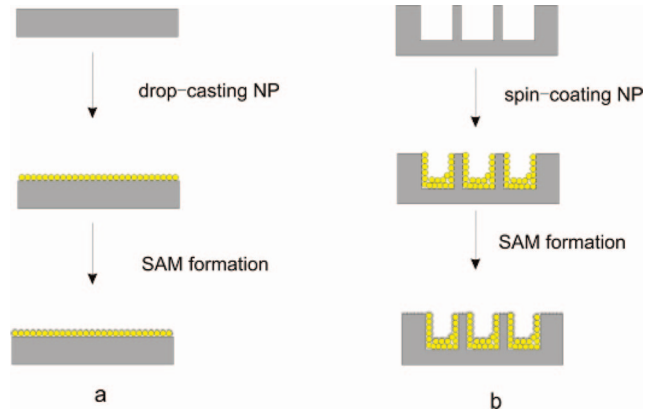

Figure 1. Schematic illustration of the coating process of nanoparticle on silicon nitride (the nanoparticles and monolayer are not in scale). (a) Drop-casting of nanoparticles followed by SAM formation. (b) Spin-coating on the pillared substrates followed by SAM formation.

CAs are interesting in that they show the contact angle differences in a dynamic regime. This dynamic contact angle difference between the advancing (θ_{adv}) and receding (θ_{rec}) CA is contact angle hysteresis and normally taken as an indication of the molecular smoothness of a substrate. For the SAMs on silicon nitride, all surfaces showed CAs greater than 90° (Table 1), indicating hydrophobic SAMs formation. Fluorinated FDTS SAM showed an average static contact angle of 110°, with $\theta_{adv}/\theta_{rec}$ = 120°/90°. The CA hysteresis is rather high, indicating that the surface is not as smooth as the other two types of SAM. Some other groups also reported that perfluorinated SAMs requires critical conditions.[21] We observed severe polymerization on the substrate. DTS showed a static contact angle of 100° with $\theta_{adv}/\theta_{rec}$ = 113°/93°, respectively. In case of an OTS SAM on silicon nitride, these values are 107° (θ), with $\theta_{adv}/\theta_{rec}$ = 115°/100°, respectively. For the latter two SAMs, CA hysteresis is about 20°, indicating a layer with good homogeneity. These two types of SAMs can be readily reproduced.

The formation of a silane SAM on silicon has been studied in great detail. However, there are only a few reports on the formation of silane SAMs on silicon nitride. Because silicon nitride can be oxidized and form a layer of silicon oxide on the surface, silanization has been achieved. For example, in 2003, our group reported the silanization and SAM formation on silicon nitride.[22] Our study showed that the quality of SAMs on silicon nitride is comparable with those silane SAMs on silicon oxide. These SAMs are very stable in that they can withstand gold atomic bombardment while their integrity is kept.

For the OTS SAM on silicon nitride, the contact angle values are very close to reported results of OTS SAM on silicon oxide with $\theta_{adv}/\theta_{rec}$ = 110°/98°,[23] indicating that our OTS SAM is well-ordered. Although perfluorinated SAM of FDTS showed the highest advancing contact angle, because of the poor layer order and reproducibility problems, we decided to choose OTS as the silanization agent for further study.

Wettability of Silica Nanoparticles Coating Silicon Nitride. The processing of silica nanoparticles as coating layers is schematically shown in Figure 1a. The particle solution was drop cast on a freshly cleaned silicon nitride substrate. This casting process could be repeated in order to obtain coatings of different thickness. After drying in the oven and OTS SAM

(20) Stober, W.; Fink, A.; Bohn, E. *J. Colloid Interface Sci.* **1968**, *26*, 62.

(21) Shaporenko, A.; Cyganik, P.; Buck, M.; Ulman, A.; Zharnikov, M. *Langmuir* **2005**, *21*, 8204.

(22) Kölbel, M.; Tjerkstra, R. W.; Kim, G.; Brugger, J.; van Rijn, C. J. M.; Nijdam, W.; Huskens, J.; Reinhoudt, D. N. *Adv. Funct. Mater.* **2003**, *13*, 219.

(23) Fadeev, A. Y.; McCarthy, T. J. *Langmuir* **2000**, *16*, 7268.

Table 2. Wetting Properties and Relative Coating Thickness of Silica-Nanoparticle-Coated Silicon Nitride Substrates

substrate	static θ (deg)	θ_{adv} (deg)	θ_{rec} (deg)	ι (nm)
a	133 ± 3	144 ± 3	135 ± 7	$-^a$
b	138 ± 3	155 ± 2	148 ± 4	144
c	140 ± 3	150 ± 2	143 ± 2	188
d	143 ± 3	154 ± 2	153 ± 1	280

[a] Determination of the exact layer thickness was not obtainable due to the transparency of silicon nitride. ι represents the layer thickness. The SAM was OTS.

Table 3. Actual Geometric Parameters of Substrates, with *d*, *p*, and *h* Representing the Pillar Diameter, Pitch, and Height, Respectively

sample	d (μm)	p (μm)	h (μm)	r^a	f^a
d1.5p2.5	1.1	2.5	0.8	1.53	0.81
d1.5p3.0	1.0	3.0	0.8	1.32	0.90
d1.5p3.5	1.1	3.5	0.8	1.26	0.91
d2.0p3.5	1.8	3.5	0.8	1.43	0.76
d2.0p4.0	1.8	4.0	0.8	1.33	0.82

[a] The roughness factor (r) was calculated by the actual surface area divided by the projected surface area. Air fraction (f) was calculated based on the actual geometry of the substrates.

formation, the water contact angle of the substrates and layer thickness were measured (Table 2). For all surfaces, the hydrophobicity is enhanced by a much higher water CA than an OTS SAM on a flat silicon nitride with static contact angles ranging from 133° to 143°. This high hydrophobicity is attributed to the roughening effect of silica nanoparticles and is in good agreement with Wenzel's prediction that roughness will enhance the hydrophobic effect.[24] The differences in the static contact angles of the substrates coated with silica nanoparticles are attributed to the thickness of the coating layers, as indicated by the ellipsometry measurements. It is, however, very difficult to obtain exact information about the thickness of the coating layer because silicon nitride is transparent to the ellipsometry laser beam. However, for thicker coatings, the relative thickness could be measured. For substrate a, the layer thickness was not measurable, due to a low coating coverage, as observed in SEM (Figure 2). Furthermore, it appeared that thicker layers correspond to higher water contact angles, which might be due to the nonideal packing of the silica nanoparticles. This nonideal packing is expected to further roughen the surface.

We used field emission scanning electron microscopy (SEM) to image the packing and coverage of the coatings (Figure 2). For substrates a, we observed that the particles did not constantly cover the surfaces. This is in good agreement with the ellipsometry data, where layer thickness was not measurable due to the incomplete coverage of the coating particles. For layers b, c, and d, the coating layers appear to be thicker. Especially for layers c and d, much thicker and denser coatings were observed. The SEM image showed that no ideal close packing was formed with many defects in the coating layer. For thicker layers, less defect spots are observed. These observations are also in good agreement with ellipsometry data.

Wettability of Silicon Nitride Substrates with Regular Asperities. A great deal of surfaces with regular asperities have been fabricated by photolithography[25–29] or micromachining. In this investigation, we used micromachining to fabricate silicon nitride substrates with circular posts in a hexagonal arrangement schematically shown in Figure 3.[30] The silicon nitride pillar arrays were prepared by chemical vapor deposition on silicon wafer, followed by classic photolithography and etching. The precise parameters of substrates determined by SEM are listed in Table 3.

In order to obtain a hydrophobic surface, the substrates were treated with piranha, rinsed with copious amounts of water, and silanized with OTS. The wetting properties of the different substrates with water are shown in Table 4. The static contact angle data indicate that all the surfaces are hydrophobic with a static contact angle ranging from 120° to 140°, approximately.

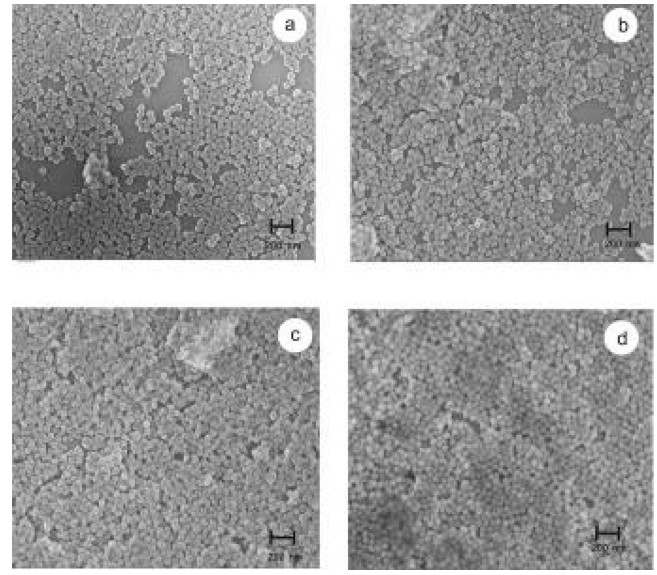

Figure 2. SEM micrographs of 60 nm silica nanoparticles coating silicon nitride substrates a, b, c, and d.

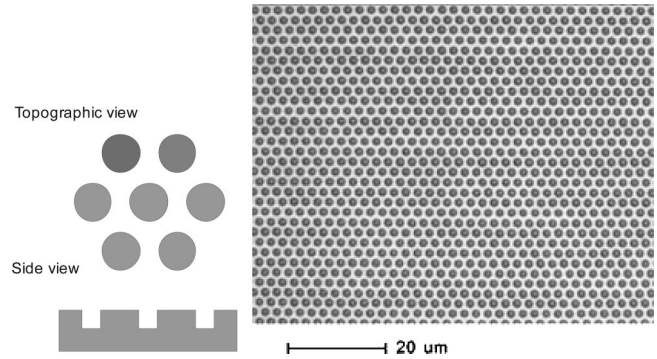

Figure 3. Schematic illustration of the patterns of the pillar arrays (left) and an optical microscope image of the pillar substrate (right, substrate d1.5p2.5, top view).

Table 4. Wettability of OTS SAM Modified Pillared Substrates

sample	static θ (deg)	θ_{adv} (deg)	θ_{rec} (deg)	$\Delta\theta$ (deg)
d1.5p2.5	$140^a/125^b$	125 ± 2	80 ± 2	45
d1.5p3.0	144 ± 2	130 ± 2	80 ± 2	50
d1.5p3.5	119 ± 2	122 ± 2	78 ± 2	44
d2.0p3.5	137 ± 2	137 ± 2	87 ± 2	50
d2.0p4.0	133 ± 2	137 ± 2	80 ± 2	57

[a] Composite state. [b] Collapsed.

(24) Wenzel, R. N. *Ind. Eng. Chem.* **1936**, *28*, 988.
(25) Furstner, R.; Barthlott, W.; Neinhuis, C.; Walzel, P. *Langmuir* **2005**, *21*, 956.
(26) Martines, E.; Seunarine, K.; Morgan, H.; Gadegaard, N.; Wilkinson, C. D. W.; Riehle, M. O. *Nano Lett.* **2005**, *5*, 2097.
(27) Oner, D.; McCarthy, T. J. *Langmuir* **2000**, *16*, 7777.
(28) Chen, W.; Fadeev, A. Y.; Hsieh, M. C.; Oner, D.; Youngblood, J.; McCarthy, T. J. *Langmuir* **1999**, *15*, 3395.
(29) Ou, J.; Perot, B.; Rothstein, J. P. *Phys. Fluids* **2004**, *16*, 4635.
(30) For unknown reasons, the shape of the pillars appeared like tubes. However, these defects do not affect the conclusion drawn, as shown by the results.

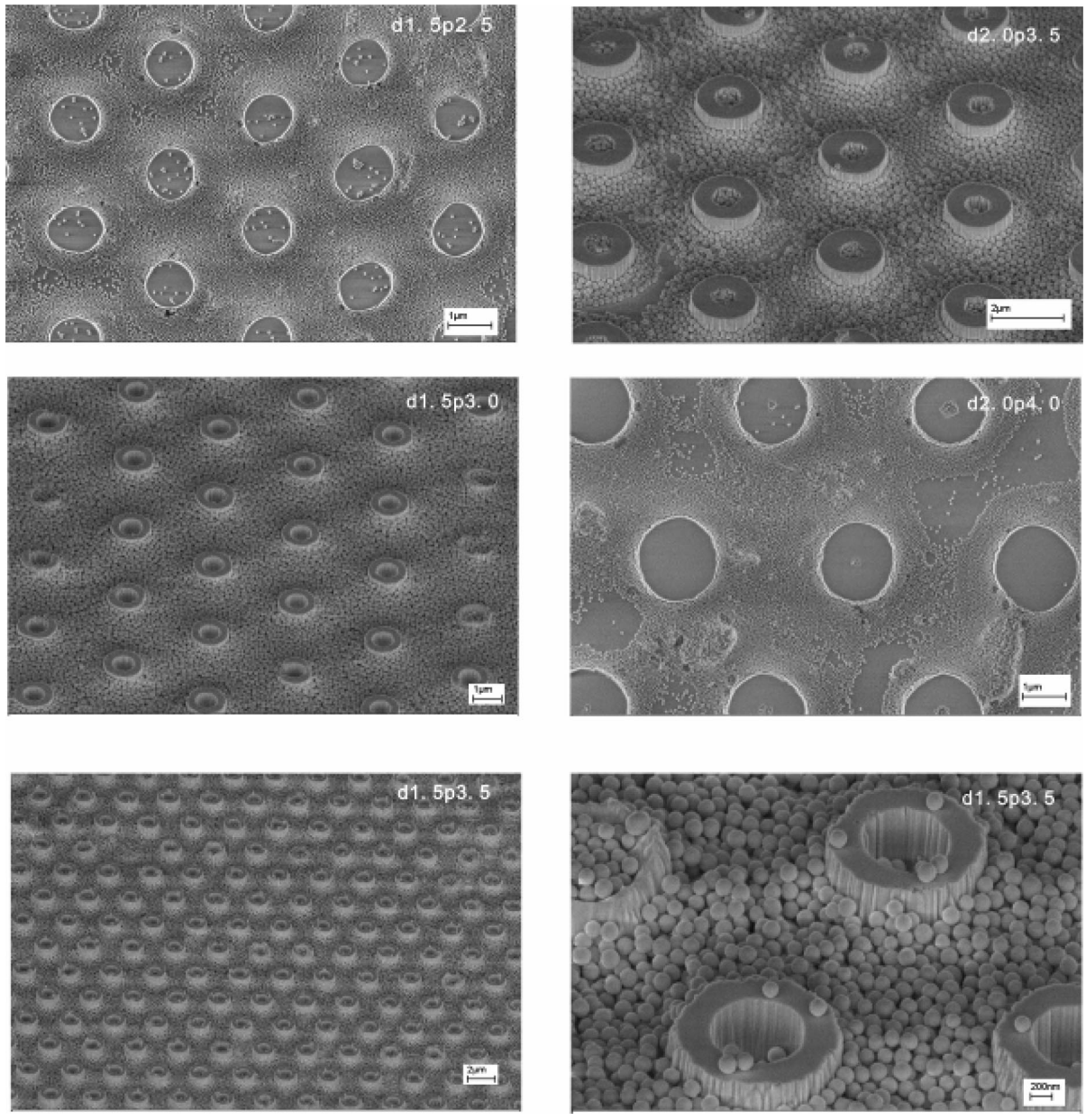

Figure 4. SEM images of substrates with two-scale roughness. In the left panel are SEM images of substrates d1.5P2.5 (10 000×), d1.5p3.0 (20 000×), and d1.5p3.5 (10 000×), respectively. In the right panel are SEM images of substrates d2.0p3.5 (25 000×), d2.0p4.0 (10 000×), and d1.5p3.5 (75 000×), respectively.

Table 5. Wettability of OTS SAM Modified Silica-Nanoparticle-Coated Pillared Substrates

sample	static θ (deg)	θ_{adv} (deg)	θ_{rec} (deg)	$\Delta\theta$ (deg)
d1.5p2.5	152.2 ± 2	156 ± 2	154 ± 2	2
d1.5p3.0	152.3 ± 2	156 ± 2	154 ± 2	1
d1.5p3.5	152.2 ± 2	152 ± 2	151 ± 2	1
d2.0p3.5	152.4 ± 2	158 ± 2	154 ± 2	4
d2.0p4.0	152.7 ± 2	155 ± 2	154 ± 2	1

The dynamic contact angle results showed that the advancing contact angles of the substrates are lower than the static contact angles (except substrate d1.5p2.5, which is clearly in Wenzel state), with huge contact angle hysteresis around 50°. Lafuma and Quere[8] have fabricated surfaces decorated with a square lattice of triangular spikes of typical height and spacing of 2 μm. It was observed that those superhydrophobic surfaces showed lower advancing contact angles than the static contact angles. They ascribed the low advancing contact angle to the instability of the metastable state. Their surfaces showed huge contact angle hysteresis, which was ascribed to the water pinning and adhesion during the dynamic measurements. Our substrates also showed lower advancing contact angles and very large contact angle hysteresis. Thus, it is evident that the substrates of our substrates are in a metastable state as well.

It should be mentioned that two static contact angles were observed for substrate d1.5p2.5. When the droplet was deposited gently on the substrates, a higher contact angle value was observed. However, with external help, for example, pressing the water droplet with a needle, the drop collapsed and a lower contact angle was observed. These two substrates clearly demonstrated the transition behavior. The higher contact angle corresponds to a water droplet suspension over the asperities and the lower contact angle is due to the pinning of the water droplet among the asperities.[6,8,9] The transition is irreversible, thus making the surfaces less superhydrophobic. How to stabilize the metastable state is a critical issue for the preparation of superhydrophobic surfaces, which will be discussed in further paragraphs.

Figure 5. A 5 μL water droplet on OTS SAM modified d1.5p3.5 substrate without (left, CA = 119°) and with 60 nm silica nanoparticles (right, CA = 152°).

Surfaces with Two-Scale Roughness. Fine-scale roughness was obtained by spin-coating the pillared substrates with 60 nm silica nanoparticles, followed by silanization (Figure 1b). SEM images of substrates with two-scale roughness revealed that the top of the pillars were not covered, and the clearance between the pillars became half-filled (Figure 4). The water contact angles of the substrates with two-scale roughness are shown in Table 5. Static contact angles of all substrates were above 150°. Compared to the wetting behavior of the pillared substrates (Table 4), substrates with two-scale roughness showed significant improvement in hydrophobicity. For example, pictures of a 5 μL water droplet on the substrate d1.5p3.5 (which was in Wenzel state) without and with two-scale roughness are shown in Figure 5. Without the nanoparticles, the CA was 119°, and after nanoparticle coating, the CA was 152°. All substrates with two-scale roughness exhibited stable wetting. No transition was observed when we applied pressure with a needle to the water droplet; rather, the water drop simply jumped to the needle. The contact angle hysteresis is much smaller than the pillared substrates that have only one-scale roughness. Apparently, application of fine-scale roughness had converted the metastable and Wenzel wetting surfaces to ultraphobic surfaces. Shirtcliffe et al.[13] reported that a surface with a double-scale roughness showed unusual water repellency. Their structures were obtained by introduction of SU 8 pillars (rough structure) on substrates with fine-scale roughness. In our method, it is observed that the apparent contact angle can be enhanced and even a metastable surface can be converted into an ultraphobic surface by the introduction of fine-scale roughness to a rough base substrate.

Surfaces with hierarchical structures have been prepared by various means, such as two-step temperature-induced capillary molding,[31] microspheres in combination with single-walled carbon nanotubes,[32] colloidal silver nanoparticles in bowl shaped structures,[16] and more.[12,19,33–37] Zhu et al.[19] have reported that fine-scale roughness reduces the contact angle hysteresis, but does not affect the contact angle itself. It was explained that the fine-scale roughness inhibits water from remaining on the surface, thus decreasing contact angle hysteresis. Similarly, Gao and McCarthy[12] have shown that fine-scale roughness reduces the contact hysteresis by introduction of a thin layer of oligosiloxane with nanoscale topography on the staggered rhombus silicon posts. From our results it is observed that the fine-scale roughness affects not only the contact angle hysteresis, but also improves the hydrophobicity of the surfaces by converting the metastable and Wenzel wetting state into an ultraphobic state. Furthermore, these results correlate well with Hermighaus's theoretical prediction[38] that small-scale roughness on the sides of larger roughness can lead to water droplet suspension. Our results have added to the literature an example of the fine-scale roughness effect in avoiding the transition state.

As mentioned before, many research groups have observed and discussed the transition state.[6,39–42] When this transition took place, the surfaces became sticky to water and contact angle hystereses also invariably turned greater than that for a flat substrate. Thus, a surface in Wenzel or metastable wetting state equals a failure in the fabrication of a superhydrophobic surface. Various methods and approaches have been proposed such as denser arrays and slender posts, which is, sometimes, practically infeasible. As both Wenzel and Cassie[43] theories are not sufficient in guiding surface design, the results presented here provided a methodology to save the failed surface design. Moreover, because the top of the pillars are not covered by the nanoparticles, this approach is potentially useful in the preparation of wear-resistant superhydrophobic surfaces.

Conclusions and Outlook

Silicon nitride substrates with microscale pillars in Wenzel and metastable state were fabricated and silanized. Hierarchical structured surfaces were obtained by application of 60 nm silica nanoparticles on the pillared substrates. It was demonstrated that application of fine-scale roughness improved significantly the surface hydrophobicity both in terms of higher apparent water contact angles and reduced contact angle hysteresis. Our results illustrated the effect of the fine-scale roughness contribution to a superhydrophobic surface and provided a new method to stabilize metastable surfaces. This is a critical issue in the fabrication of superhydrophobic surfaces.[6,39]

Acknowledgment. X.-M.L. thanks Iwan Hekamp and Jeroen Wissink at Medspray B.V. for their help in the preparation of pillared substrates and useful discussions. The Dutch Ministry of Economics Affairs, Province Overijssel, and Province Gelderland are acknowledged for the funding of the microdruppel project.

LA801044J

(31) Jeong, H. E.; Lee, S. H.; Kim, J. K.; Suh, K. Y. *Langmuir* **2006**, *22*, 1640.
(32) Li, Y.; Huang, X. J.; Heo, S. H.; Li, C. C.; Choi, Y. K.; Cai, W. P.; Cho, S. O. *Langmuir* **2007**, *23*, 2169.
(33) Nakanishi, T.; Michinobu, T.; Yoshida, K.; Shirahata, N.; Ariga, K.; Moehwald, H.; Kurth, D. G. *Adv. Mater.* **2008**, *20*, 443.
(34) Wang, M. F.; Raghunathan, N.; Ziaie, B. *Langmuir* **2007**, *23*, 2300.
(35) Xiu, Y.; Zhu, L.; Hess, D. W.; Wong, C. P. *Nano Lett.* **2007**, *7*, 3388.
(36) Lee, Y.; Park, S. H.; Kim, K. B.; Lee, J. K. *Adv. Mater.* **2007**, *19*, 2330.
(37) Zhang, F.; Low, H. Y. *Langmuir* **2007**, *23*, 7793.
(38) Herminghaus, S. *Europhys. Lett.* **2000**, *52*, 165.
(39) He, B.; Patankar, N. A.; Lee, J. *Langmuir* **2003**, *19*, 4999.
(40) Nosonovsky, M.; Bhushan, B. *Microsyst.Technol.* **2006**, *12*, 231.
(41) Nosonovsky, M.; Bhushan, B. *Microsyst. Technol.* **2006**, *12*, 273.
(42) Nosonovsky, M.; Bhushan, B. *Nano Lett.* **2007**, *7*, 2633.
(43) Cassie, A. B. D.; Baxter, S. *Trans. Farady Soc.* **1944**, *40*, 546.